A robust maximum correntropy forecasting model for time series with outliers

Jing Ren[1], Wei-Qin Li[2]

[1] College of Computer, Xi'an Aeronautical Institute, Xi'an, Shaanxi, China

[2] School of Automation and Information Engineering, Xi'an University of Technology, Xi'an Shaanxi, China

Corresponding Author:

Wei-Qin Li[1]

Jinhua South Road No.5, Xi'an, Shaanxi, 710048, China

Email address: wqlee@xaut.edu.cn

Abstract

It is of great significance to develop a robust forecasting method for time series. The reliability and accuracy of the traditional model are reduced because the series is polluted by outliers. The present study proposes a robust maximum correntropy autoregressive (MCAR) forecasting model by examining the case of actual power series of Hanzhong City, Shaanxi province, China. In order to reduce the interference of the outlier, the local similarity between data is measured by the Gaussian kernel width of correlation entropy, and the semi-definite relaxation method is used to solve the parameters in MCAR model. Results show that the MCAR model in comparison with deep learning methods, in terms of the average value of the mean absolute percentage error (MAPE), performed better by 1.63%. It is found that maximum correntropy is helpful for reducing the interference of outliers.

I. Introduction

The forecasting of the time series plays an important role in fields of natural science, social science, industrial engineering, financial science and technology and other fields. For instance, in the power system, important decisions are made on account of the forecasting results, including the generating capacity, the reliability analysis of the scheduling plan. However, under the influence of some factors, the time series has obvious variability and non-stationary (Dudek 2016), and therefore the accurate forecasting is increasingly difficult. It becomes imperative to develop the robust and effective forecasting method with higher accuracy (Fekri et al. 2021; José et al. 2019; Kong et al. 2019).

33   In the past, some machine learning methods, such as the linear regression model (Ilic et al.
34   2021), the autoregressive integrated moving average (ARIMA) model (Buyuksahin & Ertrkina
35   2019), the exponential smoothing (De Oliveria & Oliveira 2018), the grey model (Huang, Shen,
36   & Liu 2019), and the fractal extrapolation model (Wang et al. 2012), have been proposed for
37   forecasting of time series. Here, the machine learning method can establish a parameter model
38   and forecast the data in the future according to the time series data. Compared with the
39   traditional regression model, it has higher forecasting performance. Recently, some deep learning
40   models, such as the TCN-based model by incorporating calendar and weather information (Jiang
41   2022), the FF-ANNs by considering the temperature, weekends and load lags (Rajbhandari et al.
42   2021), and the RNN by BO-PSO optimizing the hyper-parameters (Li et al. 2021), are proposed
43   to improve the load forecasting performance and have higher accuracy than traditional methods.

44   However, the time series is easily polluted by the random noise and outlier, which seriously
45   reduce the reliability and accuracy of the forecasting model. For the interference of the random
46   noise, the wavelet analysis and Kalman filtering are introduced to preprocess time series (Quilty
47   & Adamowski 2018; Bashir & El-Hawary 2009; Nobrega & Oliveira 2019). Recently, the
48   empirical mode decomposition (EMD) and its improved method are applied to eliminate the
49   interference and randomness of the sequence at different time scales (Li & Chang 2018). As for
50   the outlier, it is caused by the sensor faults, the equipment failures and other unexpected events,
51   and is generally considered as the data beyond the error threshold (Dixit et al. 2021). The deep
52   learning approach (Munir et al. 2019), data preprocessing (Wang et al. 2020) and online
53   sequential outlier robust extreme learning machine (Zhang et al. 2019) are introduced to detect
54   and eliminate the outliers, which are depended on the statistical characteristics of the time series.
55   The disadvantage of the methods is that they need to set the threshold and have high time
56   complexity.

57   To solve the problem of forecasting time series polluted by outlier, a robust regression
58   model without detecting and eliminating outlier is developed in this paper. The forecasting
59   model is applicable to the complex occasions of data contaminated by outlier, especially in
60   actual industrial sites, such as electrical load forecasting, wind farm power forecasting, etc. This
61   model is expected to improve the efficiency, accuracy and robustness of time series. This paper
62   develops a robust maximum correntropy auto-regression (MCAR) forecasting model. Firstly, the
63   similarity of data is assessed by the Gaussian kernel width of correlation entropy to eliminate the
64   outlier. Then, the semi-quadratic method is presented to the quadratic programming for the

65 nonlinear non-convex programming. Lastly, in order to improve the robustness and accuracy, the

66 half a second type of the conjugate convex function and the semi-definite relaxation (SDR)

67 method are developed to estimate the model parameters.

68   The rest of the paper is organized as follows. Firstly, the robust MCAR method is

69 developed for time series with the outlier in section II. Then, the forecasting results are analyzed

70 and performances are evaluated in section III. Next, the comparison with some state of the art

71 forecasting model and discussion are presented in section IV. Moreover, the brief finding is

72 introduced in section V. Lastly, the conclusion and future directions are presented in the last

73 section.

II. Methods

1) The regression model

76   According to the linear theory, the auto-regression (AR) model of the series

77 $\hat{Y} = \{\hat{y}_1, \hat{y}_2, L \ \hat{y}_M\}$ is shown in Eq. (1)

$$\hat{y}_t = \beta_1 y_{t-1} + \beta_2 y_{t-2} + L + \beta_N y_{t-N} + e_t \tag{1}$$

79 where $\hat{y}_t, t = 1, 2, L, M$ is the forecasting load at the current moment t, M the number of group,

80 Y_{t-i} the actual load at the past moment t-i, β_i the regression parameter, e_t the error, and N the

81 regression order. Therefore, it can be expressed to Eq. (2)

$$\begin{bmatrix} \hat{y}_1 \\ \hat{y}_2 \\ M \\ \hat{y}_M \end{bmatrix} = \beta_1 \begin{bmatrix} y_0 \\ y_1 \\ M \\ y_{M-1} \end{bmatrix} + \beta_2 \begin{bmatrix} y_{-1} \\ y_0 \\ M \\ y_{M-2} \end{bmatrix} + L + \beta_N \begin{bmatrix} y_{1-N} \\ y_{2-N} \\ M \\ y_{M-N} \end{bmatrix} + \begin{bmatrix} e_1 \\ e_2 \\ M \\ e_M \end{bmatrix} \tag{2}$$

83   The least square algorithm is adopted to minimize the sum of the squares of errors (Vovk et

84 al. 2019; Midilic 2020). Let $\Phi = [\beta_1, \beta_2, L, \beta_N]$, $Z = \{z_1, z_2, L, z_M\}$ and $z_t = [y_{t-1}, y_{t-2}, L \ y_{t-N}]^T$. Eq.

85 (3) is the objective function

$$\min_{\Phi} (\hat{Y} - \Phi Z)^2 \tag{3}$$

87 Furthermore, Eq. (3) can also be written to Eq. (4)

$$\min_{\Phi} \sum_{t=1}^{M} (\hat{y}_t - \Phi z_t)^2 \tag{4}$$

89   Actually, some factors, such as the machine failure, human errors, can cause the outlier

90   point in the recording process. Consequently, the accuracy can be reduced by the above method.

91   In this work, we develop a robust regression model.

92   **2) MCAR forecasting model**

93   **a) Correntropy Analysis**

94   As shown in Eq. (4), y_t at the current moment t is calculated by the weighted sum of the data

95   of past moments. Actually, because $\hat{Y}$ and ΦZ are two random variables, the objective function

96   of Eq. (3) is the smallest if they have same statistical distributions.

97   The correntropy is the similarity measure between two random variables, as shown in Eq. (5)

$$V_\sigma(\hat{Y}, \Phi Z) = E\left[k_\sigma(\hat{Y} - \Phi Z) \right]$$

98   (5)

99   where $E[]$ is expectation. $k_\sigma(\hat{Y} - \Phi Z)$ is the Gaussian kernel as illustrated in Eq. (6)

$$k_\sigma(\hat{Y} - \Phi Z) = \exp\left(-\frac{(\hat{Y} - \Phi Z)^2}{2\sigma^2} \right)$$

100   (6)

101   where σ is a random parameter representing the kernel width, which is selected by the density

102   estimates (such as the Silverman specification).

103   In Eq. (6), the joint probability density cannot be calculated directly. Therefore, the Parzen

104   window is developed to estimate the correntropy of the limited samples

$$\hat{V}_\sigma(\hat{Y}, \Phi Z) = \frac{1}{M} \sum_{t=1}^{M} k_\sigma(\hat{y}_t - \Phi z_t)$$

105   (7)

106   where M is the number of groups as shown in Eq.(1).

107   In Eq. (7), the kernel width σ controls the window of the correntropy. Here, due to the

108   kernel width constraint and negative exponential term in Gaussian kernel, the contribution of

109   large error value to correlation entropy can be reduced. As a result, the numerical instability

110   caused by large deviation value can be avoided, and the adverse effect of outliers can be

111   effectively reduced.

112   The above method in this work compares the deviation between the output sample

113   (forecasting value) and the real sample (actual value) in the system one by one under the Gauss

114   kernel function, which is a local optimization method. However, the moment expansion

115   considers the data matrix from the whole situation and calculates the error sequence. When the

116 matrix operation is limited, it needs to construct a new calculation method, which increases the

117 algorithm complexity.

118 From geometric point of view, in the sample space, the mean square error in the least square

119 method is the 2 norm for distance, considering the second-order statistics of the data signal only,

120 and does not reflect the statistical characteristics of the data (Liu, Pokharel & Principe 2007),

121 which makes the convergence of the least squares estimation worse in non Gaussian

122 environment. Gaussian kernel function contains exponential function, and Taylor series of

123 exponential function is shown in Eq. (8)

$$e^{x^2} = 1 + x^2 + \frac{1}{2!}x^4 + \frac{1}{3!}x^6 + \frac{1}{4!}x^8 + \frac{1}{5!}x^{10} + \mathsf{L}$$

(8)

125 where x can be regarded as the element corresponding to the position in the error sequence. From

126 Eq. (8), it can be seen that the correntropy contains the even order distance. When the distance

127 between two points is close, it is equivalent to the distance measured as 2 norm. With the

128 increase of the distance, it is similar to 1 norm, or even eventually tends to 0 norm (Liang, Wang,

129 & Zeng 2015).

130 The correntropy reflects the high-order statistical characteristics and can more accurately

131 evaluate the error between the estimated value and the actual one. Therefore, it can reduce the

132 influence of outliers. In this work, the correlation entropy is introduced into the AR model to

133 enhance the robustness.

134 **b) MCAR forecasting model**

135 In the regression model, the mean square error of $\hat{Y}$ at the time t and the historical data ΦZ

136 is the quadratic function of the convex curve along a straight line $\hat{Y}=\Phi Z$. However, the value

137 away from $\hat{Y}=\Phi Z$ will increase mean error of samples, and make the regression parameters have

138 larger error in MSE.

139 Traditional mean square error is measured in the way of global similarity. All samples in the

140 joint space contribute significantly to the similarity. However, the correntropy is measured in a

141 local way. Due to locality, the value of the similarity is determined by the kernel function along

142 the line of $\hat{Y}=\Phi Z$ for random variables. Assume that $X = \hat{Y}\text{-}\Phi Z$, the Gaussian kernel function

143 of X is shown in the Fig. 1.

144 From Fig. 1, we can see that if X=0, Gaussian kernel $k_\sigma(\hat{Y}-\Phi Z)$ is maximized, and the

145 residual at the origin is zero. Here, the maximum entropy is a kind of adaptive loss function,

146 known as the maximal entropy criterion. It is suitable for the situation with non-Gaussian and

147   large outlier value (Santamaria, Pokharel & Principe 2006; Bessa, Miranda & JoÃo 2009; Chen

148   & Principe 2012; He et al. 2011). In this work, we establish a robust multidimensional regression

149   model based on the maximal entropy (MC).

150   Assume that the number of groups and order number of the model are M and N,

151   respectively. For the convenience of calculation, the equality constraint $\Phi^T\Phi = 1$ is introduced.

152   Thereby, Eq. (9) is the constraint problem on MC

$$\max_{\Phi} \sum_{t=1}^{M} k_{\sigma}(\hat{y}_t - \Phi z_t)$$

153   s.t. $\Phi^T\Phi = 1$ (9)

154   The optimization problem of Eq. (9) is nonlinear and non-convex, and cannot be solved

155   directly. The conjugate convex function is introduced to solve the semi-quadratic form. Here, the

156   auxiliary variables is introduced, and accordingly it can be simplified to Eq. (10)

$$\min_{\Phi} \sum_{t=1}^{M} \omega_t (\hat{y}_t - \Phi z_t)^2$$

157   s.t. $\Phi^T\Phi = 1$ (10)

158   Actually, the weighted function can reduce the large error term and the adverse effect of the

159   outlier on the optimization result. We define the matrix $R = \mathrm{diag}(w)$, where $w = [\omega_1, \omega_2, \mathsf{L}\ , \ \omega_M]$

160   , and hence Eq. (10) is equivalent to Eq. (11)

$$\min_{\Phi} R\left\|\hat{Y} - \Phi Z\right\|^2$$

161   s.t. $\Phi^T\Phi = 1$ (11)

162   The solution of Eq. (11) is a non-convex quadratic programming problem, which is difficult

163   to solve. When the initial condition of $R(0) = diag(1)$, Φ becomes the optimal solution, and the

164   above Eq. (11) is transformed into a homogeneous constraint programming of Eq. (12)

$$\min_{\Phi} \left\|\gamma\hat{Y} - \Phi Z\right\|^2$$
$$\text{s.t. } \gamma^2 = 1, \ \Phi^T\Phi = 1$$

165   (12)

166   It is equivalent to Eq. (13)

$$\min_{\Phi} \begin{bmatrix} \Phi^T & \gamma \end{bmatrix} \begin{bmatrix} Z^T Z & -Z^T\hat{Y} \\ -\hat{Y}^T Z & \|Z\|^2 \end{bmatrix} \begin{bmatrix} \Phi^T \\ \gamma \end{bmatrix}$$
$$\text{s.t. } \gamma^2 = 1, \ \Phi^T\Phi = 1$$

167   (13)

168   Let $\xi = [\Phi^T \ \gamma]^T$, $B = \begin{bmatrix} I_{N \times N} & 0 \\ 0 & 0 \end{bmatrix}$, and $C = \begin{bmatrix} Z^T Z & -Z^T \hat{Y} \\ -\hat{Y}^T Z & \|Z\|^2 \end{bmatrix}$. Eq. (13) can simplified to Eq. (14)

$$\min_{\Phi} \ \xi^T C \xi$$

169   s.t. $\xi^T B \xi = 1$ (14)

170   Using the semi-definite relaxation (SDR) method, the objective function and constraint

171   conditions in Eq. (14) are equivalent to Eq. (15)

$$\xi^T C \xi = \text{Tr}\{\xi^T C \xi\} = \text{Tr}\{C \xi \xi^T\}$$
$$\xi^T B \xi = \text{Tr}\{\xi^T B \xi\} = \text{Tr}\{B \xi \xi^T\}$$

172   (15)

173   where $\text{Tr}\{\}$ is the trace of the matrix. In Eq. (16), we define the matrix

$$\Omega = \xi \xi^T$$

174   (16)

175   where Ω is a symmetric positive semi-definite (PSD) matrix with a rank of 1. The resulting semi-

176   definite relaxation optimization constraint is shown in Eq. (17)

$$\min_{\Phi} \text{Tr}\{C \Omega\}$$

177   s.t. $\text{Tr}\{B \Omega\} = 1, \quad \Omega \geq 0$ (17)

178   Furthermore, let Eq. (18) is the eigen-decomposition of the matrix Ω

$$\Omega = V R V^T$$

179   (18)

180   where $V = [v_1, v_2, \text{K} \ v_M]$ is the eigenvector of Ω, and $R = \text{diag}(r_1, r_2 \text{L} \ , r_M)$ is the corresponding

181   eigenvalue. $\Omega(1) = r_1 v_1 v_1^T$ is closest to Ω when the rank is 1, and so ξ is estimated in Eq. (19)

$$\xi = \sqrt{r_1 v_1}$$

182   (19)

183   Finally, the parameter Φ is the first N value of ξ.

184   In summary, the steps of the robust MCAR forecasting method are as follows:

185   step 1): Set the maximum number of iteration, and initialize $R(0) = diag(1)$;

186   step 2): Solve the optimization constraint problem in Eq. (17) and ξ by Eq. (19);

187   step 3): According to the Silverman specification: $\sigma = 1.06 \times \min(\sigma_e, \ R/1.34) \times I^{-0.2}$ (σ_e is

188   the standard deviation of $\hat{Y} - \Phi Z$, and R is the quartile difference) get solution of ω_t;

189   step 4): Perform steps 2) and step 3) until the termination condition is reached, and find the

190   regression parameters Φ;

191   step 5): Forecast the data at the next moment based on the parameter Φ in step 4).

192   It is worth pointing out that, unlike previous methods (Bashir & El-Hawary 2009), the

193   proposed MCAR model does not need to judge whether there is outliers in the data set, but

194   directly constructs and trains the model based on the data set, since the MCAR model can

195   automatically reduce the impact of outliers by the maximal entropy.

III. Results

197   As a case study, the experimental data is taken from the actual electricity power of

198   Hanzhong City, Shaanxi province, China. Here, the time interval is 1 hour. The forecasting is a

199   one-step mode, that is, the current load is forecasted from the historical data of the past N times.

200   To analyze the forecasting performance, the root mean square error (RMSE), the mean absolute

201   error (MAE) and the mean absolute percentage error (MAPE) are employed in Eqs. (20) to (22)

202
$$RMSE = \sqrt{\frac{\sum_{i=1}^{T}(y_i - \hat{y}_i)^2}{T}} \tag{20}$$

203
$$MAE = \frac{\sum_{i=1}^{T}|y_i - \hat{y}_i|}{T} \tag{21}$$

204
$$MAPE = \frac{\sum_{i=1}^{T}\left|\frac{y_i - \hat{y}_i}{y_i}\right|}{T} \times 100\% \tag{22}$$

205   where y_i and $\hat{y}_i$ represent the actual load value and the forecasting one at the time t respectively,

206   and T is the total forecasting number.

207   Firstly, the forecasting performance of regression forecasting model is tested. Here, the

208   model order N and group number M on the accuracy are set to 4 and 8, respectively. The solution

209   method is the least square method (LSM). As shown in Fig. 2, the forecasting load curves of 4:00

210   in 15 days from January 6 to January 20 are shown respectively. It can be seen that, if the load

211   series is slow to change, the forecast error is rather low; contrarily, if the sequence has a greater

212   change (a sharp rise or drop), the forecast accuracy is rather high. This means that AR

213   forecasting model is sensitive to the sharp change of time series. Here, some effects may lead to

214   load data greater change and regression forecasting model is more sensitive to the outlier.

215   **1) Comparison of MCAR and regression models**

In this section, the performance of the proposed MCAR model is compared with the differential autoregressive (MDAR) model and AR model. Here, to guarantee a fair comparison, parameters of three methods are set to the same value as shown in Table 1. The training data sets are the same, which are taken from the January data set. Firstly, the performance of three methods on normal data (no outlier) is verified. Results of the relative errors (Re) of the 50 different forecasting points are illustrated in Fig. 3. It can be seen that, the relative error of the AR and the MDAR model have a large error at the forecasting point 7, 29 and 34, due to the sudden increase or decrease of the actual data.

Table 2 shows the corresponding performance indexes. Here, the MAPE of MCAR is 4.74%, while that of the AR and MDAR models are greater than 7%. Meanwhile, the other performance indexes of MCAR are relatively small, indicating that the proposed MCAR model is superior to the other regression models.

Next, the robustness of the MCAR model on the outlier is further verified. Fig. 4 shows the comparison of forecasting results from January 6 (day 1) to January 20 (day 15). It can be observed that, after the training sample with the outlier, the forecasting values of multiple points of AR and MDAR deviate greatly. Moreover, the results of MCAR are still good compared with the actual valuables, which mean that the proposed MCAR model in this work has higher robustness.

The comparisons of the relative errors (Re) between the forecasting result and the actual one are shown in Fig. 5. It can be seen that, AR and MDAR models have large forecasting errors. The relative error of the MCAR model remains relatively low, indicating that it is less affected by the outlier. From the performance indexes in Table 3, it can be seen that the MAPE of MCAR model is 4.88%, which is significantly smaller than that of the AR and MDAR models. In addition, compared with results with no outlier in Table 2, performance indexes did not increase significantly after the outlier data was added. This shows that, the MCAR model proposed in this work is robust to the outlier and can improve the forecasting accuracy.

2) Parameters selection of MCAR

The influences of parameter kernel width σ, model order N and group number M on the accuracy are discussed.

The influences of parameters of the Gaussian kernel on the forecasting performance are analyzed. Actually, for different data sets, the width of Gaussian kernel is different. Here, the Silverman rule is used to determinate the kernel width. The performance indexes are calculated

248 using the forecasting valuables obtained from each kernel width, compared with the Silverman

249 rule. It can be seen from Table 4 that, RMSE, MAPE and MAE of Silverman rule are smaller

250 than the corresponding valuables with other kernel width. Here, the model considers the standard

251 deviation and quartile potential difference of error sequence synthetically, realizing the

252 restriction of increasing the correntropy to the larger error estimate value, and improves the

253 robustness of the correntropy measurement method to the outlier value.

254 Then, the AICc criterion is applied to optimize the model order in this work (Chang et al

255 2018). Eq. (23) is the AICc criterion

$$AICc = T \ln RSSN + 2N + \frac{2N(N+1)}{T-N-1}$$

256 (23)

257 where T is the number of samples, and N the model order. $RSSN = \|Y - \Phi Z\|^2$ is the forecasting

258 error. Here, when T is small, the constraint ability of the AICc criterion on the number of

259 parameters is strengthened, and so it is applicable to the case that the number of samples is small

260 in this work.

261 Table 5 shows the performance indexes of the normal data and the data with the outlier with

262 different model orders. Here, the number of groups is set to 4. It can be seen that, the

263 performance indexes are smallest when the order $N=4$, which indicates that the forecasting

264 results are dependent on the model order. As shown in Table 6, the minimum value of the model

265 order is 34.07 of AICc model. Meanwhile, the optimal model order is $N=4$. This is consistent

266 with the experimental result in Table 5.

267 Lastly, the number of groups in the MCAR model is also a variable parameter which can

268 affect on the forecasting performance. Table 7 shows the performance indexes of MCAR model

269 with different groups. Here, kernel width is optimized by the Silverman rule and the model order

270 is fixed to 4. It can be seen that, whether or not the load data with the outlier, the forecasting

271 error is minimum when the number of groups is 4 in this experiment. Here, when the number of

272 groups is small, the model cannot find the similarity of load series. However, with the further

273 increase of the number of groups, the similarity of the load series decreases, and the distribution

274 difference of the time series becomes larger. It should be noted that, the optimal number of

275 groups is different for different data sets. Thereby, in the actual modeling process, the number of

276 groups needs to be selected according to the characteristics of the dataset.

277 **IV. Discussion**

278   In this section, the performance of the proposed model is compared with some state of the

279   art deep learning methods which have been applied for load forecasting, including adaptive

280   recurrent neural networks (Adaptive RNN), long short term memory (LSTM) networks, gated

281   recurrent units (GRU) and the combination model. The training samples in this section are taken

282   from the power series from January to November, and the test samples from December. Settings

283   of some parameters are shown in Table 8. To guarantee a fair comparison, the valuables of

284   parameters of deep learning methods networks (Adaptive RNN, LSTM, and GRU) are set to

285   same valuables, where these have been optimized. Here, the parameters of Adaptive RNN are set

286   as recommended in Ref. (Fekri et al. 2021). The algorithm of LSTM is based on Ref. (Kong et

287   al. 2019). The algorithm of GRU are based on Ref. (Li et al. 2020). Parameters of the

288   combination model are set based on Ref. (Li and Chang 2018).

289   The performance indexes of the series with the outlier are tabulated in Table 9. The results

290   show that, the proposed MCAR model displays promising results in terms of the average values

291   of MAPE, MAE, and RMSE indexes for the series with the outlier, although LSTM produces

292   less value for the normal data. As for the maximum values of MAPE, MAE, and RMSE indexes,

293   the MCAR model also produces smaller values due to less sensitive to the outlier. Moreover, the

294   MCAR model has less training times in comparison with deep learning methods, since it only

295   need several training samples and contrarily deep learning methods need a large number of

296   training samples and accordingly more computing time.

297   Finally, the uniqueness and novelty of this work is introduced. The established MCAR

298   model can automatically eliminate the influence of outliers without detecting outliers. The local

299   similarity between the true value and the regression one is measured by the maximum correlation

300   entropy, which reduces outlier in the optimization solution of regression model. Average value

301   of MAPE can be reduced to 1.63% in comparison with some state of the art method (Adaptive

302   RNN, LSTM, GRU, and combination model). However, the traditional methods need to use

303   filtering methods, such as statistical learning methods and wavelet analysis, to detect outliers and

304   set thresholds which are depended on the statistical characteristics of the series, and therefore

305   have high time complexity.

V. Findings

307   The advantages and limitations of the proposed MCAR model are analyzed in this section.

308   The model is a robust regression model that can automatically eliminate outlier interference. It

309 does not need to detect outliers of time series and to set thresholds, which effectively improves
310 the accuracy, efficiency and reliability. Therefore, it is suitable for online forecasting of time
311 series disturbed by outliers and noises. Moreover, different from the deep learning model which
312 requires a large number of training samples, the MCAR model only needs a small number of
313 (number groups) data to train model, but it is unable to discover more information implied in the
314 data set. Also, it is difficult to determine the optimal number of groups in the modeling process,
315 and it can only be selected according to experience. How to optimize the number of groups is our
316 further research content.

317 VI. Conclusions

318 This study has established a robust MCAR forecasting model for the time series with outlier.
319 The local similarity between data is measured by the Gaussian kernel width of maximum
320 correlation entropy. Therefore, the MCAR model reduces the sensitivity to the outlier and
321 enhances the accuracy and robustness. The advantage is that there is no need to detect outlier and
322 set thresholds. The average values of MAPE, MAE and RMSE indexes and the training time of
323 MCAR model are decreased in comparison with deep learning methods. However, it should be
324 pointed out that, external factors, such as weather and holidays, have not been considered in our
325 model. In future, the forecasting model should incorporate the calendar, weather information, the
326 temperature, workday and weekends to furthermore improve the forecasting performance. This is
327 also our next research direction.

328 Acknowledgements

329 The authors would like to thank Dr. Junli Liang, Professor of Northwestern Polytechnical
330 University, for helpful advice. This work was supported by the National Natural Science
331 Foundation of China under grant no. 61871318.

332 References

333 **Bashir ZA, El-Hawary ME.** 2009. Applying wavelets to short-term load forecasting
334 using PSO-based neural networks. *IEEE Transaction on Power System* **24**(1):20-27
335 **Bessa RJ, Miranda V, JoÃo G.** 2009. Entropy and correntropy against minimum
336 square error in offline and online three-day ahead wind power forecasting. *IEEE
337 Transactions on Power Systems* **24**(4):1657-1666

338 **Buyuksahin UC, Ertrkina S.** 2019. Improving forecasting accuracy of time series data
339 using a new ARIMA-ANN hybrid method and empirical mode decomposition.
340 *Neurocomputing* **361**:151-163

341 **Chang LL, Zhou ZJ, Chen YW, Xu XB, Sun JB, Liao TJ, Tan X**. 2018. Akaike
342 information criterion-based conjunctive belief rule base learning for complex system
343 modeling. *Knowledge-Based System*s **161**(1):47-64

344 **Chen B, Principe JC.** 2012. Maximum correntropy estimation is a smoothed MAP
345 estimation. *IEEE Signal Processing Letters* **19**(8):491-494

346 **De Oliveria EM, Oliveira FLC.** 2018. Forecasting mid-long term electric energy
347 consumption through bagging ARIMA and exponential smoothing methods. *Energy*
348 **144**(3):776-788

349 **Dixit P, Bhattacharya P, Tanwar S, Gupta R.** 2022. Anomaly detection in autonomous
350 electric vehicles using AI techniques: A comprehensive survey. *Expert Systems*.
351 **39**(5):e12754

352 **Dudek G.** 2016. Pattern-based local linear regression models for short-term load
353 forecasting. *Electric power systems research* **130**(1):139-147

354 **Fekri MN, Patel H, Grolinger K, Sharma V.** 2021. Deep learning for load forecasting
355 with smart meter data: online adaptive recurrent neural network. *Applied Energy*
356 **282**(A):116177

357 **He R, Hu BG, Zheng WS, Kong XW.** 2011. Robust principal component analysis
358 based on maximum correntropy criterion. *IEEE Transactions on Image Processing*
359 **20**(6):1485-1494

360 **Huang YS, Shen L, Liu H.** 2019. Grey relational analysis, principal component analysis
361 and forecasting of carbon emissions based on long short-term memory in China.
362 *Journal of Cleaner Production* **209**(1):415-423

363 **Ilic I, Gorgulu B, Cevik M, Baydogan MG.** 2021. Explainable boosted linear
364 regression for time series forecasting. *Pattern Recognition* **120**:108144

365 **Jiang W.** 2022. Deep learning based short-term load forecasting incorporating calendar
366 and weather information. *Internet Technology Letters* **5**(4): e383

367 **José FT, Alicia T, Irena K, Zheng W, Francisco MÁ.** 2019. Big data solar power
368 forecasting based on deep learning and multiple data sources. *Expert Systems*
369 **36**(4):e12394

370 **Kong W, Dong ZY, Jia Y, Hill DJ, Xu Y, Zhang Y.** 2019. Short-term residential load
371   forecasting based on LSTM recurrent neural network. *IEEE Transactions on Smart*
372   *Grid* **10**(1):841-851

373 **Li CS, Tang G, Xu, XM, Saeed A, Hu X.** 2020. Short-term wind speed interval
374   prediction based on ensemble GRU model. *IEEE Transactions on Sustainable*
375   *Energy* **11**(3):1370-1380

376 **Li WQ, Chang L.** 2018. A combination model with variable weight optimization for short
377   term electrical load forecasting. *Energy* **164**(24):575-593

378 **Li Y, Zhang Y, Cai Y.** 2021. A new hyper-parameter optimization method for power load
379   forecast based on recurrent neural networks. *Algorithms* **14**(6): 163

380 **Liang JL, Wang YL, Zeng XJ.** 2015. Robust ellipse fitting via half-quadratic and
381   semidefinite relaxation optimization. *IEEE Transactions on Image Processing* **24**(11):
382   4276-4286

383 **Liu W, Pokharel PP, Principe JC.** 2007. Correntropy: properties and applications in
384   non-Gaussian signal processing. *IEEE Transactions on Signal Processing*
385   **55**(11):5286-5298

386 **Midilic M.** 2020. Estimation of STAR-GARCH models with iteratively weighted least
387   squares. *Computational Economics* **55**(1):87-117

388 **Munir M, Siddiqui SA, Dengel A, Ahmed S.** 2019. DeepAnt: A deep learning
389   approach for unsupervised anomaly detection in time series. *IEEE Access* **7**:1991-
390   2005

391 **Nobrega JP, Oliveira ALI.** 2019. A sequential learning method with Kalman filter and
392   extreme learning machine for regression and time series forecasting.
393   *Neurocomputing* **337**(4):235-250

394 **Quilty J, Adamowski J.** 2018. Addressing the incorrect usage of wavelet-based
395   hydrological and water resources forecasting models for real-world applications with
396   best practices and a new forecasting framework. *Journal of Hydrology* **563**:336-353

397 **Rajbhandari Y, Marahatta A, Ghimire B, Shrestha A, Gachhadar A, Thapa A,**
398   **Chapagain K, Korba P.** 2021. Impact study of temperature on the time series
399   electricity demand of urban nepal for short-term load forecasting. *Applied System*
400   *Innovation* **4**(3): 43

401 **Santamaria I, Pokharel PP, Principe JC.** 2006. Generalized correlation function:
402   definition, properties, and application to blind equalization. *IEEE Transactions on*
403   *Signal Processing* **54**(6):2187-2197

404 **Vovk V, Shen JL, Manokhin V, Xie MG.** 2019. Nonparametric predictive distributions
405   based on conformal prediction. *Machine Learning* **108**(3):445-474

406 **Wang JZ, Jia RL, Zhao WG, Wu J, Dong Y.** 2012. Application of the largest Lyapunov
407   exponent and non-linear fractal extrapolation algorithm to short-term load forecasting.
408   *Chaos Solitons & Fractals* **45**(9):1277-1287

409 **Wang JZ, Du P, Hao Y, Ma X, Niu T, Yang WD.** 2020. An innovative hybrid model
410   based on outlier detection and correction algorithm and heuristic intelligent
411   optimization algorithm for daily air quality index forecasting. *Applied Mechanics &*
412   *Materials* **255**(2):109855

413 **Zhang D, Peng XG, Pan KD, Liu Y.** 2019. A novel wind speed forecasting based on
414   hybrid decomposition and online sequential outlier robust extreme learning machine.
415   *Energy Conversion and Management* **180**:338-357

Figure 1

Gaussian kernel function with different variables
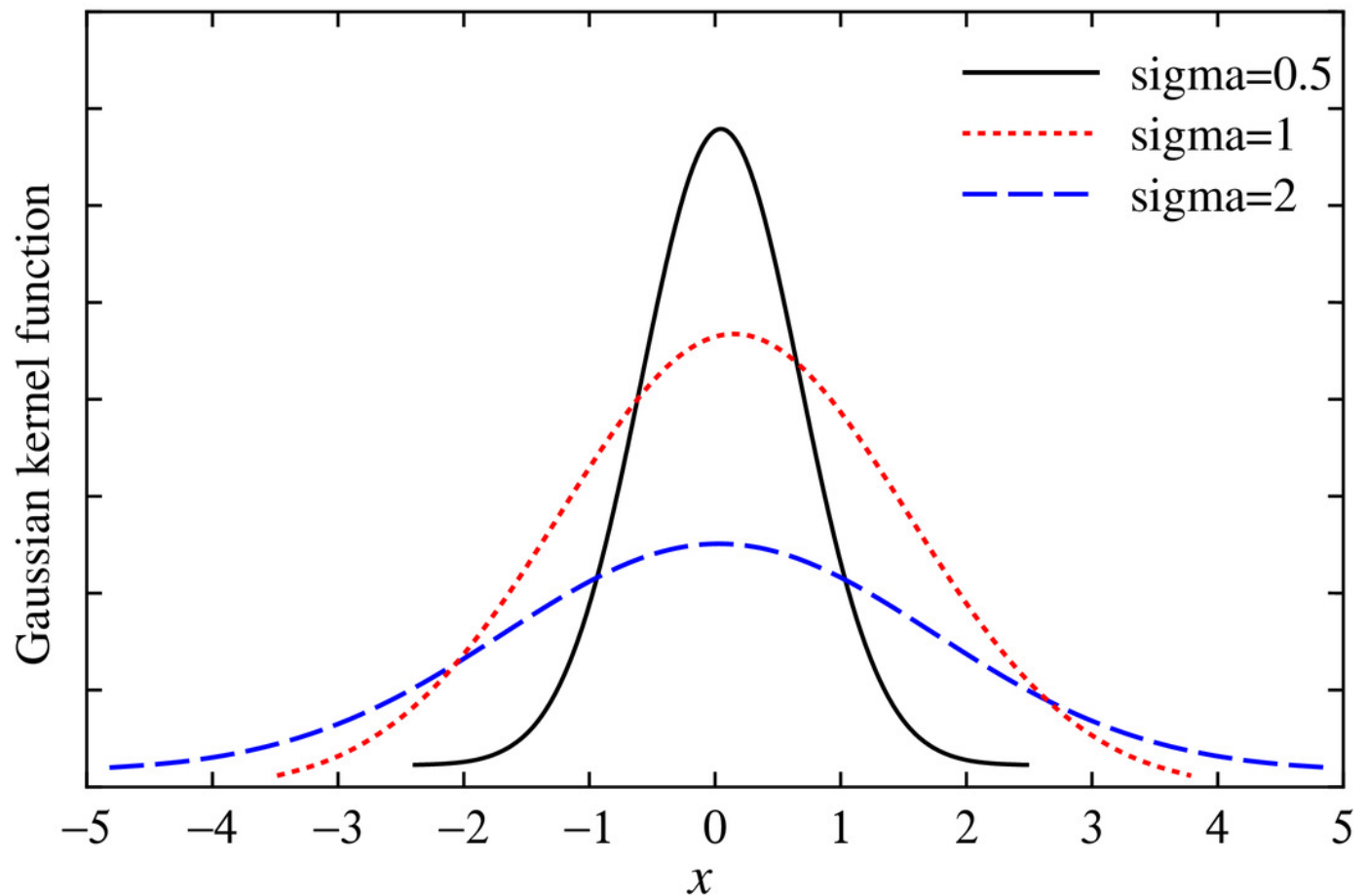
Figure 2

The forecasting results by regression model at 4:00 from January 6 to 20

The solid and dot curves indicate that the actual loads and the forecasting results, respectively.
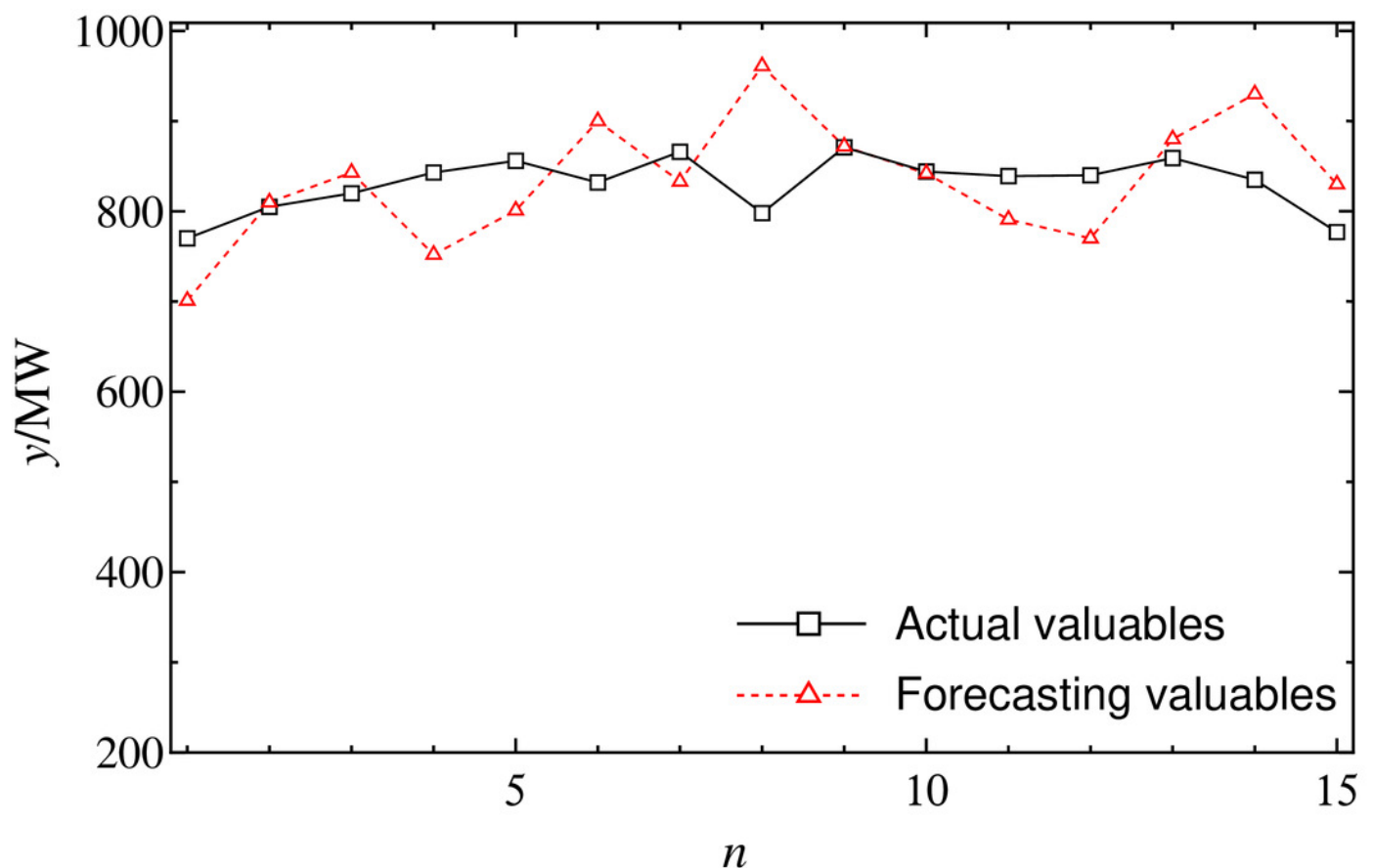
Figure 3

Comparison of the forecasting relative errors of normal data (no outlier)

The solid, dash, and dot-dash curves are the relative errors of the outlier data of MCAR, MAR, and MDAR, respectively.
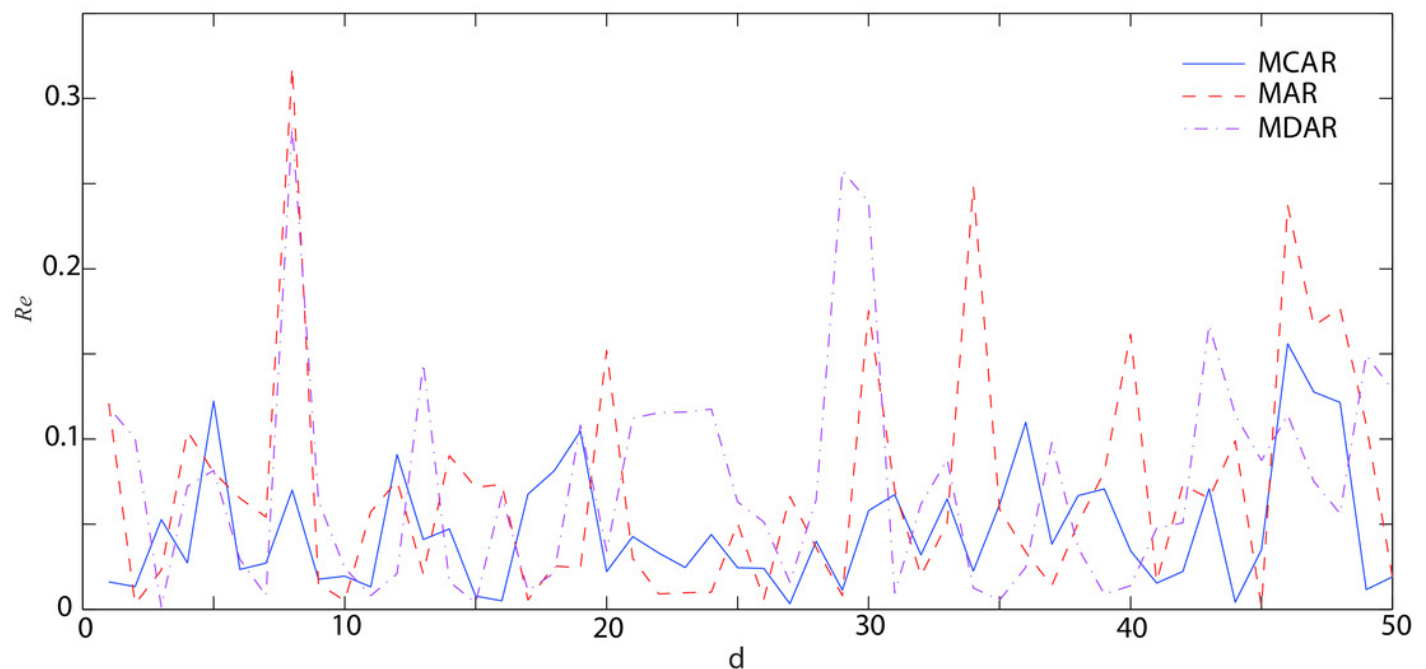
Figure 4

Comparison of the forecasting results with outlier data at 4:00 from January 6 to 20

The dot, dash, and dot-dash curves show the forecasting results of MCAR, MAR, and MDAR, respectively.
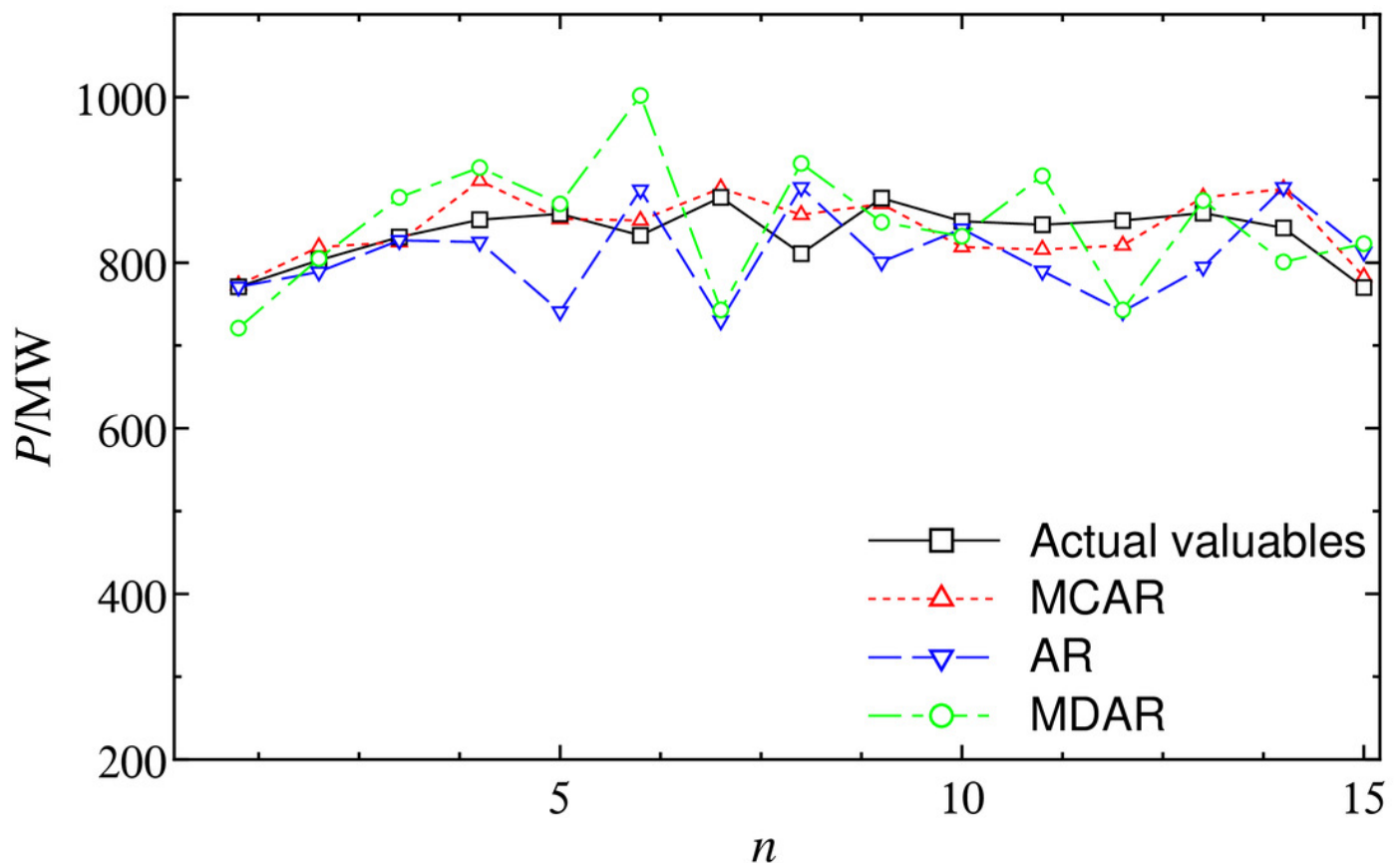
Figure 5

Comparison of the forecasting relative errors of data with the outlier

The solid, dash, dot-dash curves are the relative errors of MCAR, MAR, and MDAR, respectively.
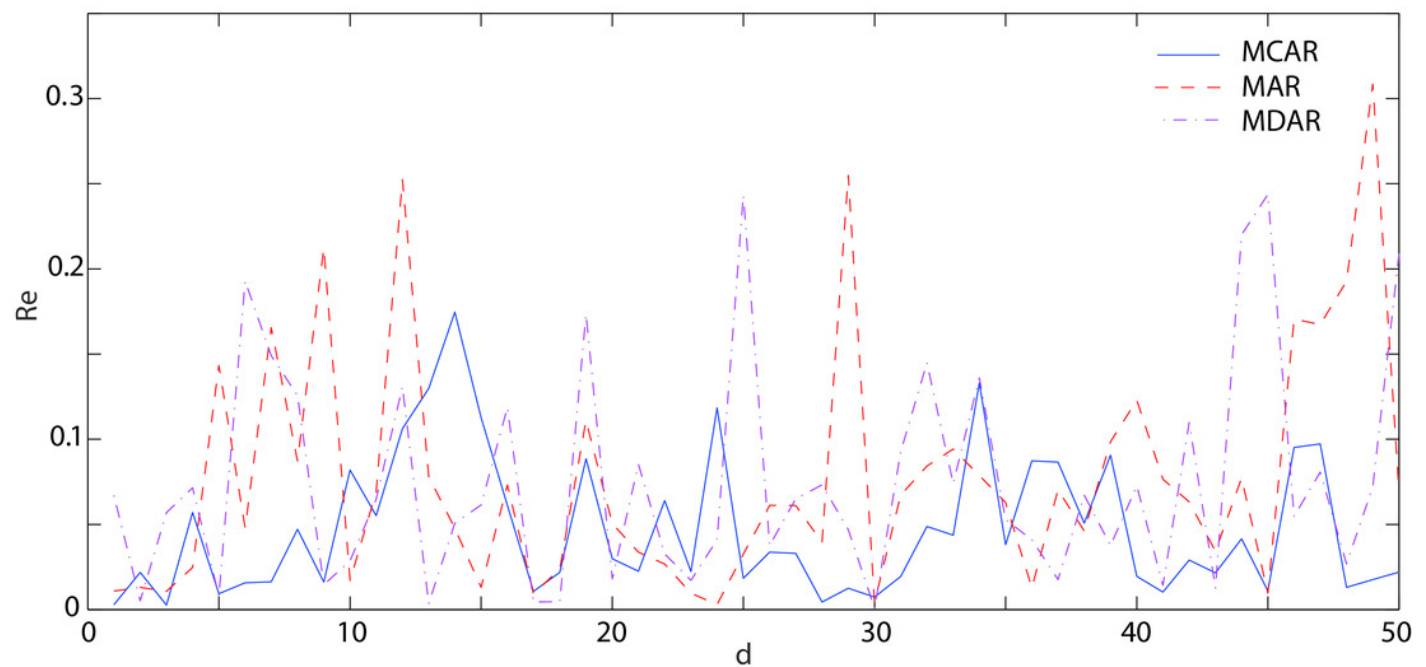
Parameters setting of forecasting models.

Parameters	Forecasting models		
	AR	MDAR	MCAR
Solution method	LSM	LSM	LSM
Model order	4	4	4
Group number	8	8	8
Kernel width	-	-	1000

Performance indexes of the normal data of MCAR, AR and MDAR models

Performance indexes	Forecasting models		
	AR	MDAR	MCAR
RMSE(MW)	85.213	84.032	54.015
MAPE(%)	7.08	7.44	4.74
MAE(MW)	60.727	63.695	40.964

Performance indexes of AR, MDAR and MCAR with outlier data.

Performance indexes	Forecasting model		
	AR	MDAR	MCAR
RMSE (MW)	92.783	84.818	56.655
MAPE(%)	7.79	7.55	4.88
MAE (MW)	67.752	64.500	41.952

Performance indexes of MCAR with different kernel sizes

Kernel size	Performance indexes		
	RMSE(MW)	MAPE(%)	MAE(MW)
1000	316.704	14.25	119.954
1200	317.115	14.55	122.516
1500	81.285	7.98	67.884
2000	181.499	11.71	98.329
2500	102.938	10.62	91.065
Silverman	63.058	4.18	44.412

Comparison of performance indexes of different model orders

Tha data indicate the performance indexes of the normal data and the data with the outlier of different model orders. The performance indexes are smallest when the order $N=4$.

Model order	Performance indexes (no outliers)			Performance indexes (with outliers)		
	RMSE(MW)	MAPE(%)	MAE(MW)	RMSE(MW)	MAPE (%)	MAE(MW)
3	53.593	0.0504	42.282	63.808	0.0598	49.889
4	**53.499**	**0.0474**	**40.964**	**56.655**	**0.0488**	**41.952**
5	86.611	0.0693	62.569	83.532	0.0742	65.976
6	85.198	0.0648	67.063	90.767	0.0644	68.483

RSSN and AICc values of different model orders

The data indicate the AICc and RSSN with different model orders. The optimal model order is $N=4$.

Model order	3	**4**	5	6	7
RSSN	143.28	**25.26**	53.02	250.34	239.57
AICc	40.52	**34.07**	48.77	74.51	86.22

Comparison of performance indexes of different numbers of groups

The data indicate the performance indexes of MCAR model with different groups. The forecasting error is minimum when the number of groups is 4.

Group number	Performance indexes (no outlier)			Performance indexes (with outlier)		
	RMSE(MW)	MAPE(%)	MAE(MW)	RMSE(MW)	MAPE(%)	MAE(MW)
3	58.347	5.21	42.782	59.095	5.06	43.776
4	**54.015**	**4.74**	**40.964**	**56.655**	**4.88**	**41.952**
5	64.902	5.44	46.819	71.249	6.19	53.212
6	57.934	5.55	44.742	65.724	5.85	48.166
7	63.685	5.66	50.003	74.157	6.26	57.016

Parameters setting of forecasting models

Combinational model	Adaptive RNN, LSTM, GRU
Individual model: ARIMA, Elman, similarity model	Number of layers: 2
Optimization algorithm: CPSO	Number of training samples:8760
Knowledge capacity: 5	Optimization algorithm: Adam
$\omega_{max}, \omega_{min}$: 2, 0	Maximum number of iterations: 3000
c_1, c_2: 2.5, 0.5	Number of neurons in the hidden layer: 50
m_C, m_I: 2	Learning rate: 0.01
n_C, n_I: 5	Batch size: 40
Model order: 5	Bidirectional: No

Comparisons of performance indexes of studied forecasting models

The data show the performance indexes of the series with the outlier of some forecasting models. The proposed MCAR model displays promising results in terms of the average values of MAPE, MAE, and RMSE indexes.

Performance Indexes		Forecasting models				
		Adaptive RNN	LSTM	GRU	Combination model	MCAR
RMSE (MW)	Averages	79.562	77.683	79.006	81.329	56.655
	Minimum	1.587	1.492	1.556	1.920	1.620
	Maximum	150.041	149.478	153.275	154.451	107.358
MAPE(%)	Averages	6.625	6.442	6.840	7.424	4.880
	Minimum	0.123	0.097	0.088	0.111	0.079
	Maximum	9.072	8.743	9.518	11.389	7.961
MAE (MW)	Averages	58.669	56.504	59.774	61.502	41.952
	Minimum	1.590	1.511	1.685	2.227	1.365
	Maximum	94.074	93.258	93.662	118.468	79.347
Training time (s)	-	746	767	253	96	26